Designing Charge Carrier and Exciton Dynamics for Efficient Organic Long-Persistent Luminescence

Rengo Yoshioka,[a] Liliia Moshniaha,[a] Ryota Kabe*,[a]

[a]Organic Optoelectronics Unit, Okinawa Institute of Science and Technology Graduate University, 1919-1 Tancha, Onna-son, Okinawa, 904-0495, Japan. E-mail: ryota.kabe@oist.jp

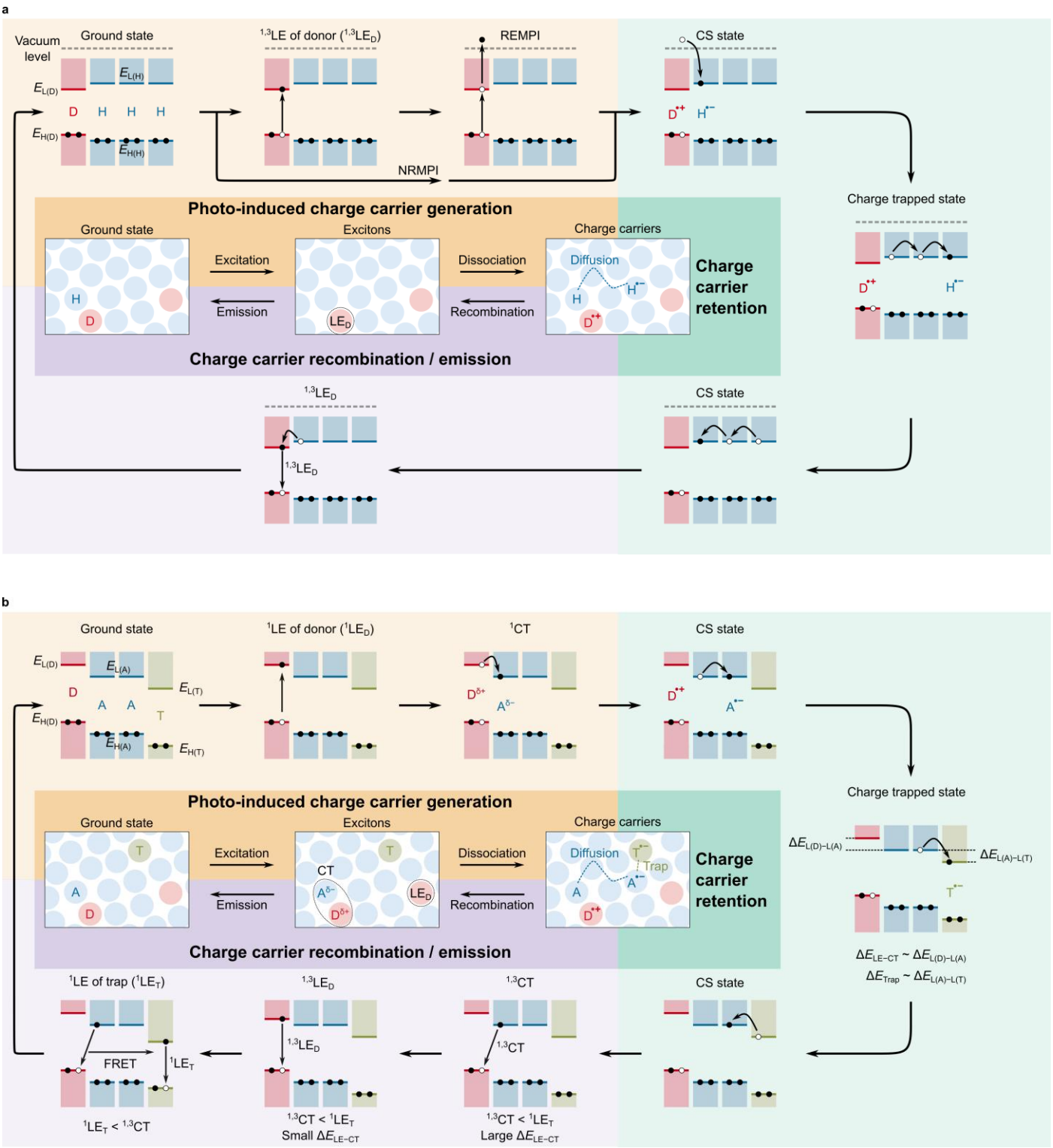

Supplementary Fig. 1 | Mechanism of multiphoton ionization-mediated OLPL and electron-diffusion type OLPL.

a, Schematic illustration of the multiphoton ionization-mediated OLPL mechanism, showing charge carrier generation, retention, and recombination between donor (D) and host (H) molecules. E_L, LUMO energy level; E_H, HOMO energy level; ^{1}LE, ^{3}LE, singlet, triplet locally excited states; REMPI, resonance-enhanced multiphoton ionization; NRMPI, nonresonant multiphoton ionization; CS, charge-separated. **b,** Schematic illustration of the OLPL mechanism in an electron-diffusion system, showing charge carrier generation, retention, and recombination between donor (D), acceptor (A), and trap (T) molecules. E_L, LUMO energy level; E_H, HOMO energy level; ^{1}LE, ^{3}LE, singlet, triplet locally excited states; ^{1}CT, ^{3}CT, singlet, triplet charge-transfer excited states; CS, charge-separated.

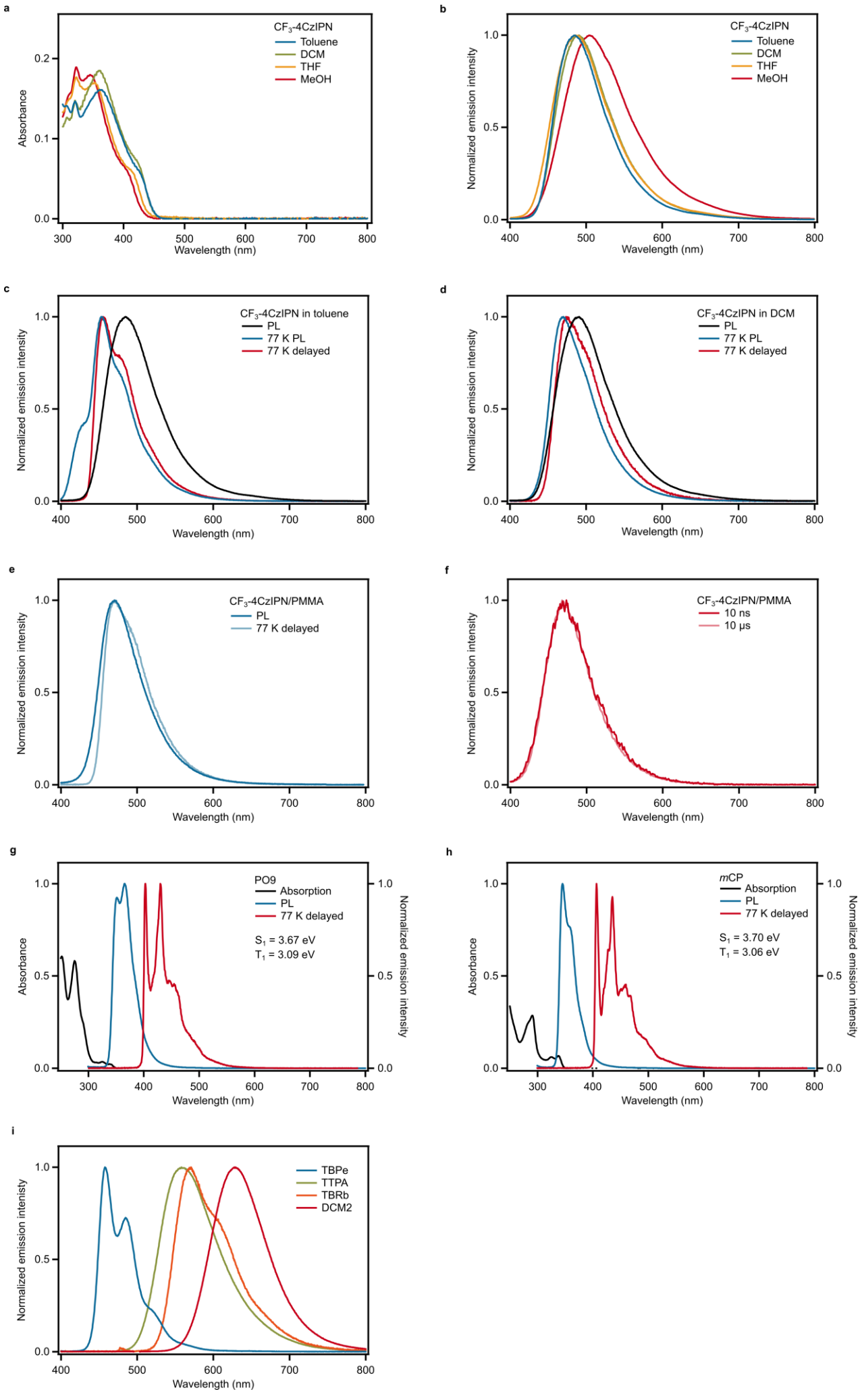
a
CF3-4CzIPN
Toluene
DCM
THF
MeOH
Absorbance
Wavelength (nm)
b
CF3-4CzIPN
Toluene
DCM
THF
MeOH
Normalized emission intensity
Wavelength (nm)
c
CF3-4CzIPN in toluene
PL
77 K PL
77 K delayed
Normalized emission intensity
Wavelength (nm)
d
CF3-4CzIPN in DCM
PL
77 K PL
77 K delayed
Normalized emission intensity
Wavelength (nm)
e
CF3-4CzIPN/PMMA
PL
77 K delayed
Normalized emission intensity
Wavelength (nm)
f
CF3-4CzIPN/PMMA
10 ns
10 µs
Normalized emission intensity
Wavelength (nm)
g
PO9
Absorption
PL
77 K delayed
S1 = 3.67 eV
T1 = 3.09 eV
Absorbance
Normalized emission intensity
Wavelength (nm)
h
mCP
Absorption
PL
77 K delayed
S1 = 3.70 eV
T1 = 3.06 eV
Absorbance
Normalized emission intensity
Wavelength (nm)
i
TBPe
TTPA
TBRb
DCM2
Normalized emission intensity
Wavelength (nm)

Supplementary Fig. 2 | UV-vis absorption and photoluminescence properties of molecules.

a, UV–vis absorption spectra of CF_3-4CzIPN in various solvents (1.0×10^{-5} M). **b,** Steady-state photoluminescence (PL) spectra of CF_3-4CzIPN in various solvents. **c,** Steady-state PL spectrum at room temperature (PL), steady-state PL spectrum at 77 K (77 K PL) and delayed emission spectrum at 77 K (77 K delayed) of CF_3-4CzIPN in toluene (1.0×10^{-5} M). **d,** PL, 77 K PL and 77 K delayed spectra of CF_3-4CzIPN in DCM (1.0×10^{-5} M). **e,** PL and 77 K delayed spectra of CF_3-4CzIPN/PMMA film (excitation: 365 nm LED; PL under nitrogen atmosphere; 77 K delayed spectra were obtained in liquid nitrogen). **f,** Time-resolved photoluminescence spectra of CF_3-4CzIPN/PMMA film (excitation: 365 nm laser, 300 K, under vacuum). **g,** UV-vis absorption and emission spectra (PL and 77 K delayed) of PO9 in DCM solution (1.0×10^{-5} M). **h,** UV-vis absorption and emission spectra (PL and 77 K delayed) of *m*CP in DCM solution (1.0×10^{-5} M). **i**, PL spectra of TBPe (excitation: 410 nm), TTPA (excitation: 470 nm), TBRb (excitation: 480 nm) and DCM2 (excitation: 500 nm) in DCM solutions (1.0×10^{-5} M). PL spectra were measured at room temperature. All 77 K delayed spectra were recorded with a delay time of 100 ms.

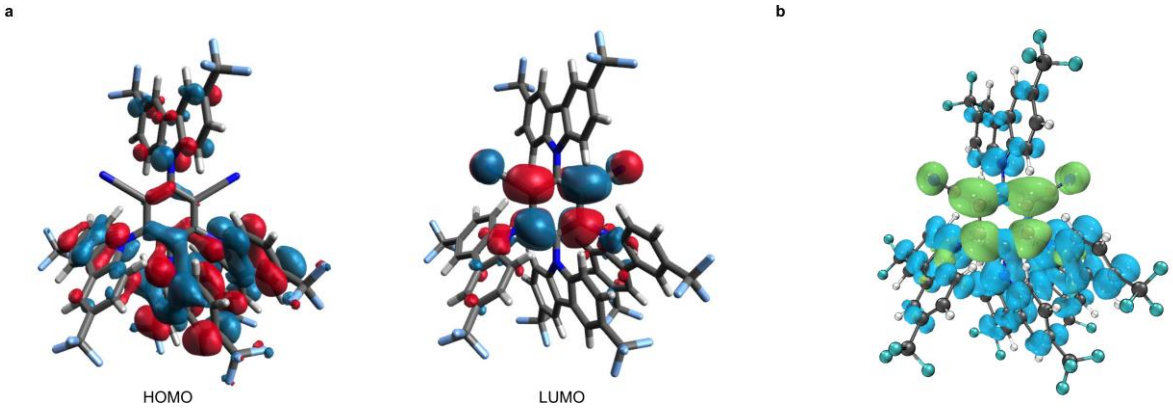

Supplementary Fig. 3 | Quantum chemical calculation of CF_3-4CzIPN.

a, Frontier molecular orbitals (HOMO and LUMO) of CF_3-4CzIPN (isovalue = 0.02). **b,** Hole-electron analysis of CF_3-4CzIPN at S_1 state (isovalue = 0.0005). Blue and green isosurfaces represent hole and electron distributions, respectively.

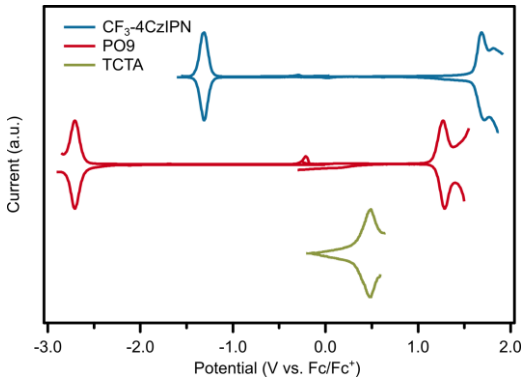

Supplementary Fig. 4 | Differential pulse voltammetry of CF_3-4CzIPN, PO9 and TCTA.

All measurements were performed in super-dehydrated acetonitrile (ACN) containing 0.1 M tetrabutylammonium hexafluorophosphate as the supporting electrolyte, with a compound concentration of 0.5 mM. Due to the low solubility in ACN, TCTA was measured using a saturated solution (< 0.5 mM). The reduction peak of TCTA was not clearly observed under these conditions. Therefore, the LUMO energy level was estimated from the reported HOMO-LUMO gap.[1] The HOMO and LUMO energy levels of *m*CP, TBPe, TTPA, TBRb and DCM2 were adopted from our previous reports.[2,3]

Supplementary Table 1 | Photoluminescence quantum yields of CF_3-4CzIPN in solution and film.

Steady-state photoluminescence quantum yields (PLQY) of solutions (1.0×10^{-5}M) and melt-casted films (1/99 or 1/99/1 molar ratios) under nitrogen atmosphere. Samples were excited at 360 nm.

Sample	PLQY	Absorbance at 360 nm
CF_3-4CzIPN in toluene	76%	0.620
CF_3-4CzIPN in DCM	92%	0.638
CF_3-4CzIPN in THF	77%	0.622
CF_3-4CzIPN in MeOH	46%	0.592
CF_3-4CzIPN/PMMA	88%	0.384
CF_3-4CzIPN/*m*CP	19% (CT: 11%)	0.192
CF_3-4CzIPN/PO9	71%	0.585
CF_3-4CzIPN/PO9/TCTA	20%	0.697
CF_3-4CzIPN/PO9/TBPe	38%	0.656
CF_3-4CzIPN/PO9/TTPA	41%	0.426
CF_3-4CzIPN/PO9/TBRb	41%	0.528

Supplementary Table 2 | Lifetimes of prompt and delayed components of CF_3-4CzIPN films.

Prompt and delayed emission lifetimes of CF_3-4CzIPN/PO9, CF_3-4CzIPN/*m*CP and CF_3-4CzIPN/PMMA obtained from exponential fitting to transient decay profiles (excitation: 365 nm laser; 300 K; under vacuum). Emission was integrated across the 400–800 nm region.

Sample	Lifetime	
	Prompt (ns)	Delayed (μs)
CF_3-4CzIPN/PO9	6.0	4.4
CF_3-4CzIPN/*m*CP	2.4	3.0
CF_3-4CzIPN/PMMA	5.4	4.1

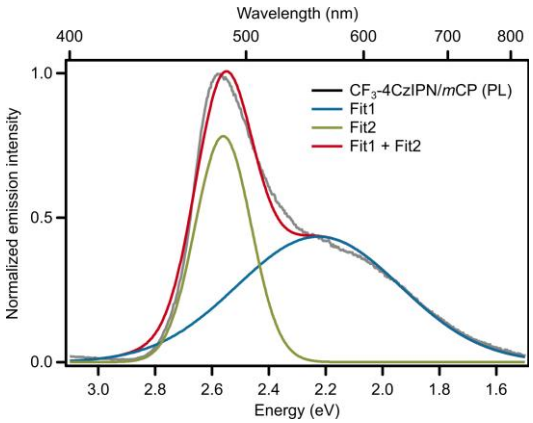

Supplementary Fig. 5 | Two-component Gaussian fitting of the CF_3-4CzIPN/*m*CP PL spectrum.

The steady-state PL spectrum was converted from wavelength to energy representation using a Jacobian transformation[4] and subsequently fitted with two Gaussian functions and a constant baseline:

$$f(x) = a_1 \cdot exp\left(-\frac{(x-\mu_1)^2}{2\cdot\sigma_1^2}\right) + a_2 \cdot exp\left(-\frac{(x-\mu_2)^2}{2\cdot\sigma_2^2}\right) + b_0$$

The fitted parameters (± one standard deviation) are: a_1 = 0.43442 ± 0.00576, μ_1 = 2.2254 ± 0.00611, σ_1 = 0.28747 ± 0.00712, a_2 = 0.78217 ± 0.0108, μ_2 = 2.5604 ± 0.000638, σ_2 = 0.098176 ± 0.0012 and b_0 = -0.00026698 ± 0.00498. The integrated areas of the two Gaussian components were 0.313 (assigned to the CT emission) and 0.192 (assigned to the LE emission), respectively. The area ratio was used to estimate the relative contribution of intermolecular CT emission in the CF_3-4CzIPN/*m*CP film.

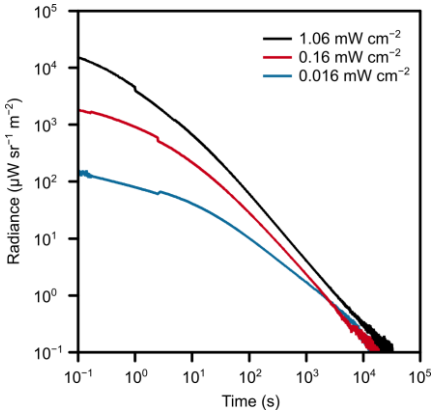

Supplementary Fig. 6 | Excitation power dependence on LPL of CF_3-4CzIPN/PO9 film.

LPL decay profiles of CF_3-4CzIPN/PO9 film (excitation: 365 nm; different power; 60 s; 300 K; under nitrogen).

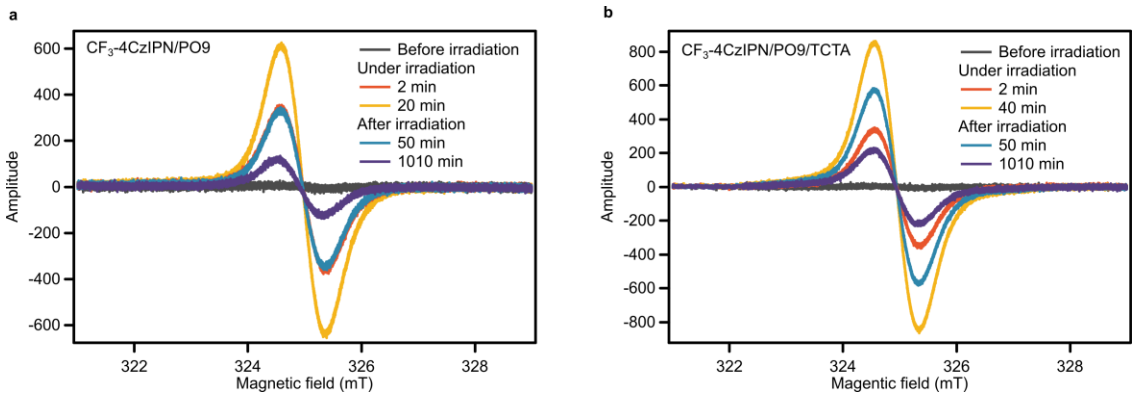

Supplementary Fig. 7 | ESR spectra of CF_3-4CzIPN/PO9 and CF_3-4CzIPN/PO9/TCTA.

ESR spectra of **a,** CF_3-4CzIPN/PO9 and **b,** CF_3-4CzIPN/PO9/TCTA before, during, and after UV photoexcitation. Samples were irradiated with a 365 nm LED light until signal saturation, followed by continuous measurements after irradiation.

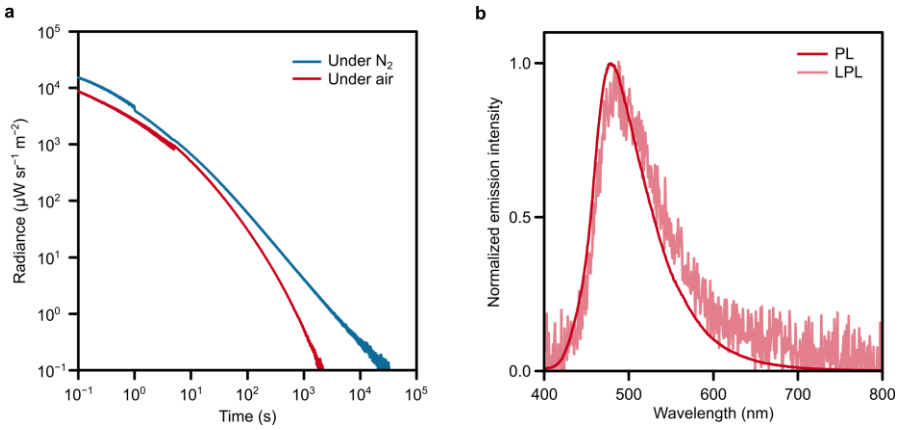

Supplementary Fig. 8 | LPL decay profiles of CF_3-4CzIPN/PO9 film under ambient conditions.

a, Emission decay profiles of CF_3-4CzIPN/PO9 films measured under nitrogen and ambient air after photoexcitation (365 nm; 1.06 mW cm^{-2}; 60 s; 300 K). **b,** Steady-state PL, LPL spectra of CF_3-4CzIPN/PO9 film under air (excitation: 365 nm; 300 K). Before measurement in air, the sample was exposed to air for 24 h without exposure to light.

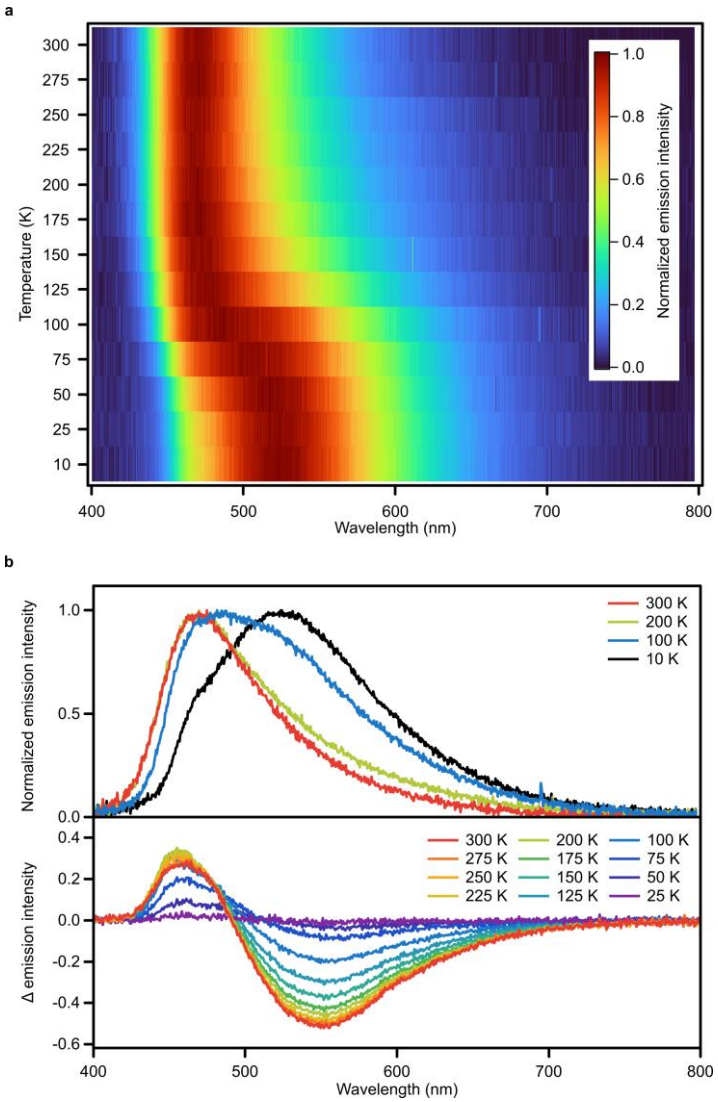

Supplementary Fig. 9 | Temperature dependent LPL spectra of CF_3-4CzIPN/PO9 film.

a, Two-dimensional map showing the evolution of the LPL spectrum as a function of temperature. **b,** LPL spectra at selected temperatures (top) and difference spectra for all temperatures (bottom). The difference spectra were obtained by subtracting the normalized 10 K spectrum from each normalized spectrum. recorded 10 s after cessation of excitation (365 nm LED, 180 s) under vacuum.

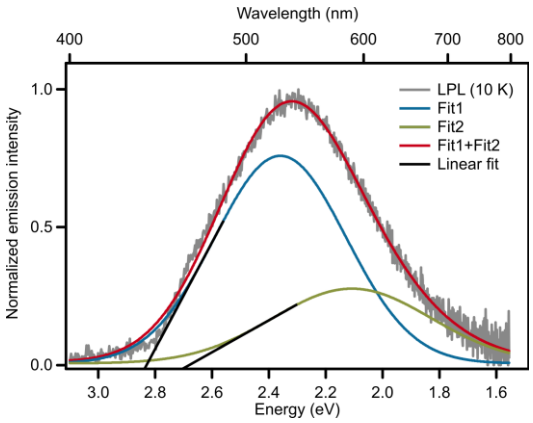

Supplementary Fig. 10 | Two-component Gaussian fitting of the CF_3-4CzIPN/PO9 LPL spectrum measured at 10 K.

The LPL spectrum at 10 K was converted from wavelength to energy representation using a Jacobian transformation,[4] normalized, and subsequently fitted with two Gaussian functions and a constant baseline:

$$f(x) = a_1 \cdot exp\left(-\frac{(x-\mu_1)^2}{2\cdot\sigma_1^2}\right) + a_2 \cdot exp\left(-\frac{(x-\mu_2)^2}{2\cdot\sigma_2^2}\right) + b_0$$

The fitted parameters (± one standard deviation) are: $a_1 = 0.75313 \pm 0.706$, $\mu_1 = 2.3593 \pm 0.0451$, $\sigma_1 = 0.23138 \pm 0.0228$, $a_2 = 0.27099 \pm 0.528$, $\mu_2 = 2.1078 \pm 0.494$, $\sigma_2 = 0.27853 \pm 0.126$ and $b_0 = 0.011929 \pm 0.00195$. The obtained two Gaussian curves are then fitted with linear functions to determine the energies of the LE and CT excited states.

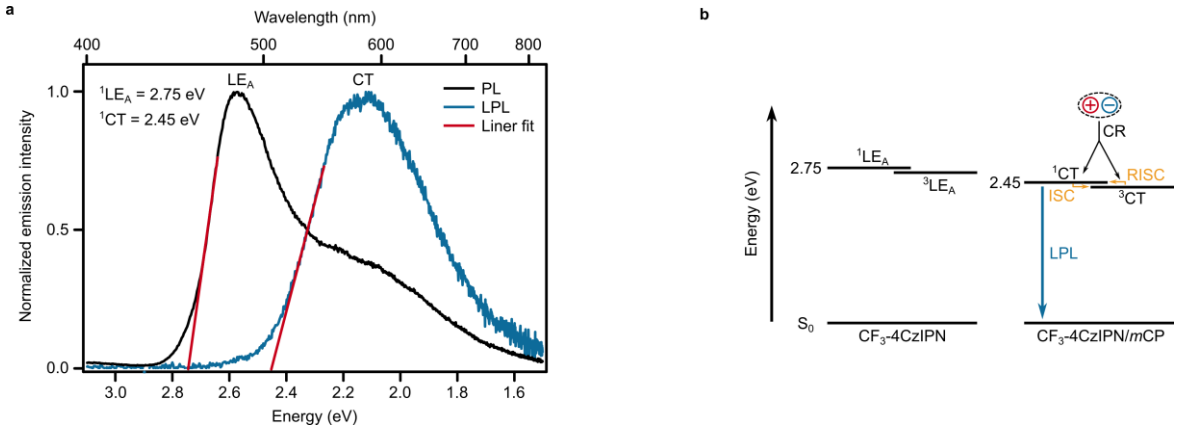

Supplementary Fig. 11 | Excited-state energies of CF_3-4CzIPN/*m*CP.

a, Normalized steady-state PL and LPL spectra of a CF_3-4CzIPN/*m*CP film. The spectra were converted from wavelength to energy representation using a Jacobian transformation, normalized, and fitted with linear functions to determine the energies of the LE and intermolecular CT excited states. **b,** Emission mechanism of CF_3-4CzIPN/*m*CP system.

a

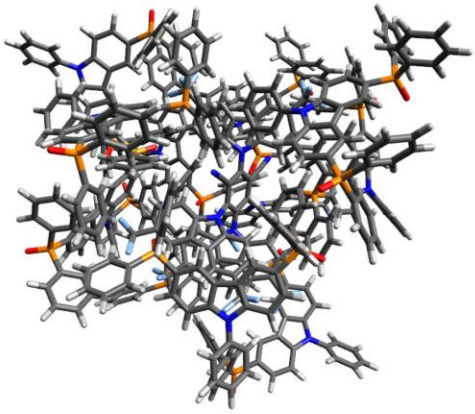

b

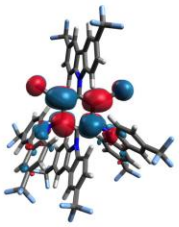

LUMO
−1.364 eV

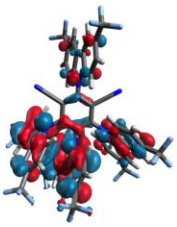

HOMO
−8.228 eV

c

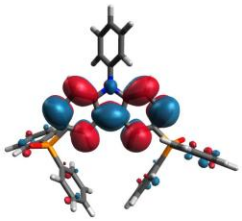

LUMO
0.521 eV

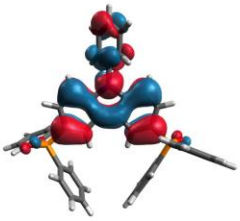

HOMO
−7.781 eV

d

	LUMO	HOMO	HOMO−1	HOMO−2
Pair 1	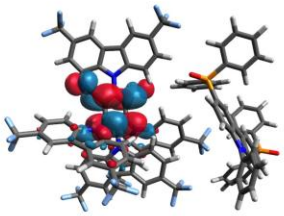 −1.376 eV	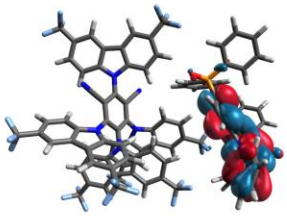 −7.753 eV	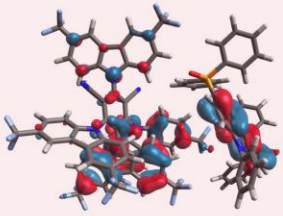 −8.161 eV	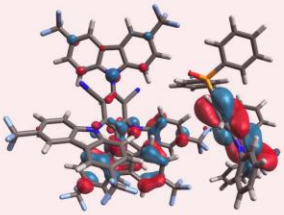 −8.172 eV
Pair 2	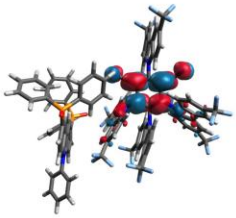 −1.372 eV	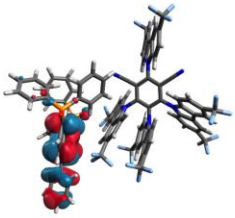 −7.629 eV	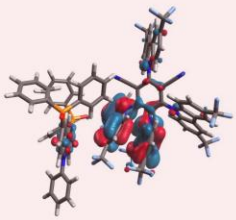 −8.076 eV	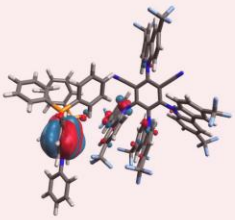 −8.127 eV
Pair 3	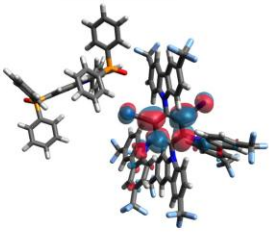 −1.372 eV	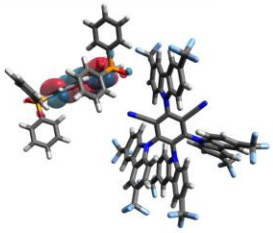 −7.687 eV	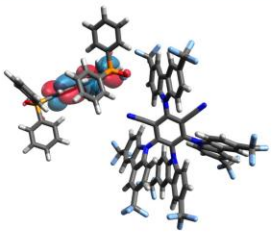 −8.121 eV	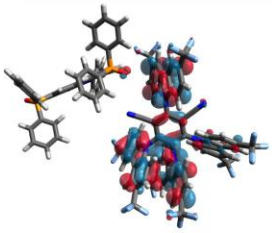 −8.134 eV
Pair 4	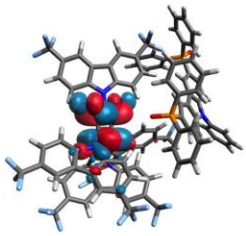 −1.263 eV	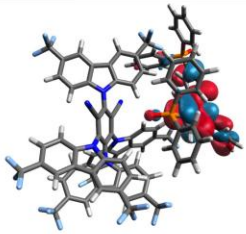 −7.675 eV	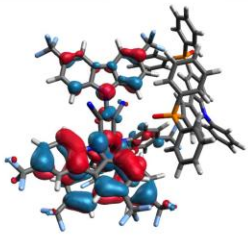 −8.125 eV	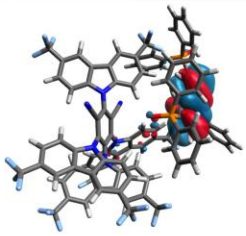 −8.245 eV

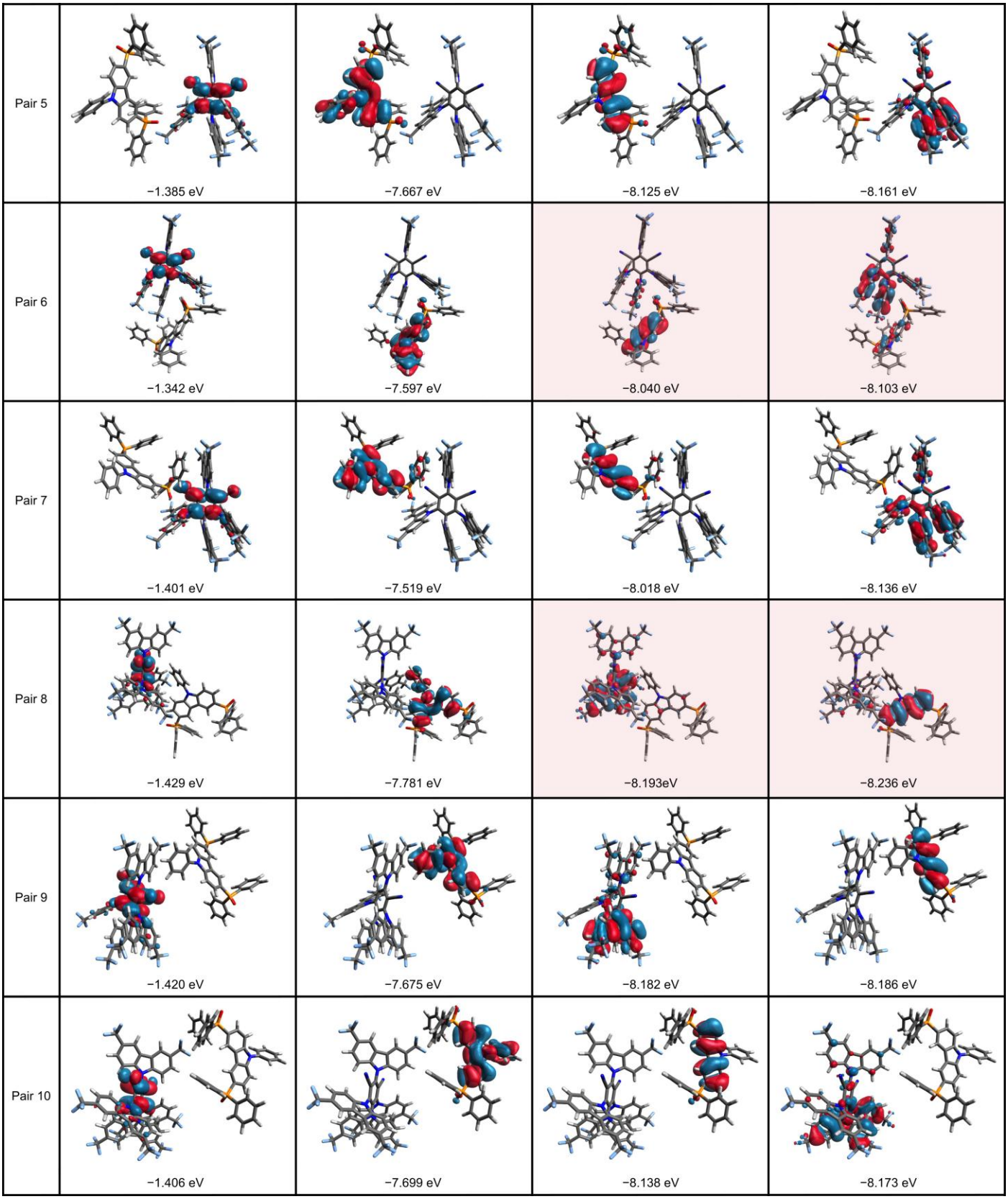

Supplementary Fig. 12 | Electronic-structure calculations of CF_3-4CzIPN/PO9 pairs.

a, A representative cluster used for the electronic-structure calculations. **b,** Molecular orbitals (LUMO, HOMO, isovalue = 0.02) of CF_3-4CzIPN. **c,** Molecular orbitals (LUMO, HOMO, isovalue = 0.02) of PO9. **d,** Molecular orbitals (LUMO, HOMO, HOMO−1 and HOMO−2, isovalue = 0.02) of CF_3-4CzIPN/PO9 pairs extracted from the molecular cluster consisted of one CF_3-4CzIPN and ten PO9. The hybridized MOs are highlighted with a red background. Calculations were performed at the ωB97X-D/6-31G(d,p) level of theory.

Supplementary Table 3 | Calculated excited-state properties of CF3-4CzIPN/PO9 molecular pairs.

TD-DFT results for the CF_3-4CzIPN/PO9 molecular pairs, including the vertical excitation energy of the first singlet excited state (E_{S1}), oscillator strength (f), and dominant orbital contributions (>10%) to the transition. Transitions involving hybridized molecular orbitals are highlighted in red. Calculations were performed at the ωB97X-D/6-31G(d,p) level of theory.

Molecular pair	E_{S1} (eV)	f	Orbital composition
Pair 1	3.50	0.1451	HOMO–1→LUMO (47%) HOMO–2→LUMO (29%) HOMO–3→LUMO (13%)
Pair 2	3.44	0.1597	HOMO–1→LUMO (67%) HOMO–3→LUMO (13%)
Pair 3	3.48	0.1462	HOMO–2→LUMO (81%)
Pair 4	3.55	0.1451	HOMO–1→LUMO (75%) HOMO–3→LUMO (13%)
Pair 5	3.49	0.1558	HOMO–2→LUMO (70%) HOMO–3→LUMO (18%)
Pair 6	3.47	0.1388	HOMO–2→LUMO (60%) HOMO–3→LUMO (21%)
Pair 7	3.43	0.1666	HOMO–2→LUMO (72%) HOMO–3→LUMO (15%)
Pair 8	3.48	0.1335	HOMO–1→LUMO (64%) HOMO–3→LUMO (15%)
Pair 9	3.48	0.1420	HOMO–1→LUMO (69%) HOMO–3→LUMO (18%)
Pair 10	3.49	0.1390	HOMO–2→LUMO (69%) HOMO–3→LUMO (19%)

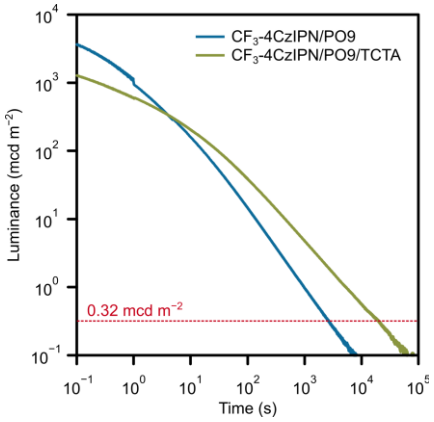

Supplementary Fig. 13 | LPL decay profile of the CF_3-4CzIPN/PO9 and CF_3-4CzIPN/PO9/TCTA films plotted in units of luminance.

Emission decay profiles of two-component CF_3-4CzIPN/PO9 and three-component CF_3-4CzIPN/PO9/TCTA films in units of luminance (excitation: 365 nm; 1.06 mW cm^{-2}; 60 s; 300 K; under nitrogen). A luminance level of 0.32 mcd m^{-2} is the standard threshold used for comparing LPL duration and corresponds to 100 times the lower limit for light perception by the dark-adapted human eye.

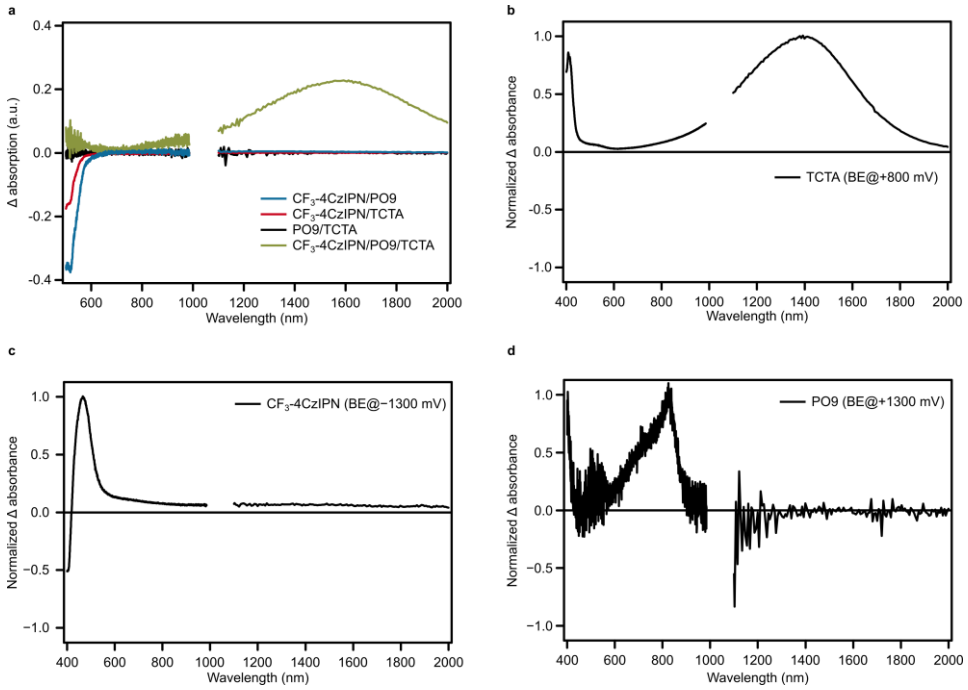

Supplementary Fig.14 | Differential absorption spectra of solutions and films.

a, Differential absorption spectra of CF_3-4CzIPN/PO9, CF_3-4CzIPN/TCTA, PO9/TCTA and CF_3-4CzIPN/PO9/TCTA films before and after photoexcitation (365 nm LED; 300 K; under nitrogen). Normalized differential absorption spectrum of **b,** TCTA; **c,** CF_3-4CzIPN; and **d,** PO9 solutions containing tetrabutylammonium hexafluorophosphate as the supporting electrolyte, measured during bulk electrolysis (BE).

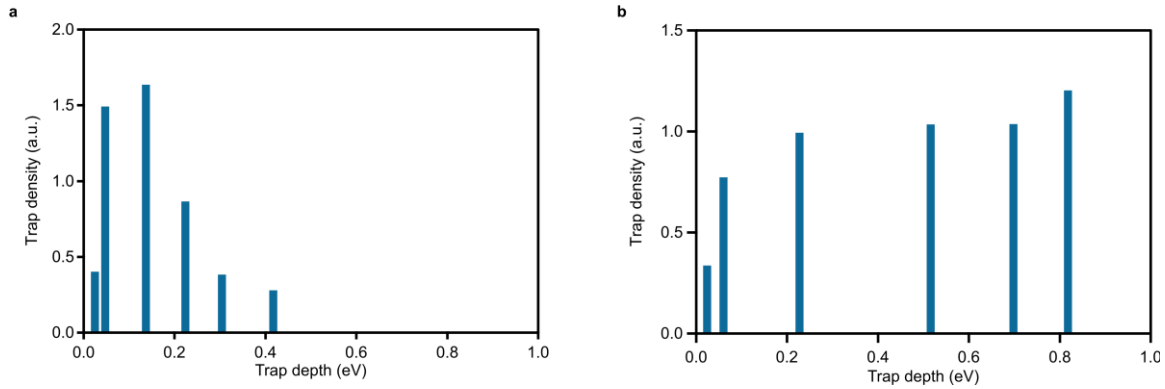

Supplementary Fig. 15 | Trap depth distribution of CF_3-4CzIPN films.

Trap depth distribution estimated using the initial rise method[5,6] from the TSL glow curve for **a**, CF_3-4CzIPN/PO9 and **b**, CF_3-4CzIPN/PO9/TCTA.

Supplementary References

1. Jinnai, K., Kabe, R., Lin, Z. & Adachi, C. Organic long-persistent luminescence stimulated by visible light in p-type systems based on organic photoredox catalyst dopants. *Nat. Mater.* **21**, 338–344 (2022).
2. Oyama, R. *et al.* Investigating charge accumulation mechanisms in organic materials via slow transient emission spectroscopy. *Sci. Adv.* **11**, eadx9806 (2025).
3. Jinnai, K., Kabe, R. & Adachi, C. Wide-range tuning and enhancement of organic long-persistent luminescence using emitter dopants. *Adv. Mater.* **30**, e1800365 (2018).
4. Mooney, J. & Kambhampati, P. Get the basics right: Jacobian conversion of wavelength and energy scales for quantitative analysis of emission spectra. *J. Phys. Chem. Lett.* **4**, 3316–3318 (2013).
5. McKeever, S. W. S. & Yukihara, E. G. *Optically Stimulated Luminescence: Fundamentals and Applications*. (Wiley-Blackwell, Hoboken, NJ, 2011).
6. Van den Eeckhout, K., Bos, A. J. J., Poelman, D. & Smet, P. F. Revealing trap depth distributions in persistent phosphors. *Phys. Rev. B* **87**, 045126 (2013).